The 15th International Symposium on District Heating and Cooling

On the influence of thermally induced radial pipe extension on the axial friction resistance

Tim Gerlach[a,*], Martin Achmus[a]

[a]Gottfried Wilhelm Leibniz University of Hannover, Institute for Geotechnical Engineering (IGtH), Appelstr. 9A, 30167 Hannover, Germany

Abstract

Within the design process of district heating networks, the maximum friction forces between the pipeline and the surrounding soil are calculated from the radial stress state and the coefficient of contact friction. For the estimation of the radial stresses, the soil unit weight, geometric properties such as the pipe's diameter and the depth of embedment, as well as the groundwater level are taken into account. For the coefficient of contact friction, different values are proposed, dependent on the thermal loading condition of the pipeline. Although this is an assumption of practical use, physically the coefficient of friction is a material constant.

To revise the interaction behavior of the soil-pipeline system with respect to thermally induced radial pipe extension, a two-dimensional finite element model has been developed. Here, the frictional contact was established using Coulomb's friction law. For the embedment, sand at different states of relative density was considered. This noncohesive, granular material was described by the constitutive model HSsmall, which is able to predict the complex non-linear soil behavior in a realistic manner by stress-dependency of stiffness as well as isotropic frictional and volumetric hardening. In addition to the basic Hardening Soil model, the HSsmall model accounts for an increased stiffness in small strain regions, which is crucial for the presented investigation.

After a model validation, a parametric study was carried out wherein a radial pipe displacement was applied due to thermal changes of the transported medium. Different combinations of geometry and soil property were studied. We conclude by presenting a corrective term that enables for an incorporation of thermal expansion effects into the prediction of the maximum friction force.

© 2017 The Authors. Published by Elsevier Ltd.
Peer-review under responsibility of the Scientific Committee of The 15th International Symposium on District Heating and Cooling.

Keywords: Soil-structure interaction; numerical modeling; buried pipelines, radial extension

---

* Corresponding author. Tel.: +49 511 762 3529; fax: +49 511 762 5105.
    E-mail address: gerlach@igth.uni-hannover.de

1. Introduction

In operation, a district heating pipeline is subjected to loads resulting from changes of the medium temperature. Beside the temperature rise of the transported medium, usually water, the inner pressure also varies. The stress state around the pipeline is affected by the resulting loading condition, leading to a higher maximum friction resistance under axial pipeline displacement. In common design practice in Germany [1], the maximum friction resistance is estimated from:

$$F_{max} = \mu * (F_N' + F_G') .$$
(1)

Herein F_{max} denotes the maximum resistance force per meter length, μ is the coefficient of contact friction and F_N' and F_G' are the integrated normal stresses around the pipes circumference and the sum weight force of the filled pipeline, respectively. To incorporate the effects resulting from changes of operating temperature, the coefficient of contact friction is taken to $\mu = 0.4$ for increasing temperature conditions. During unloading (decrease of temperature), a value of $\mu = 0.2$ shall be applied [1]. However, the coefficient of contact friction is a material specific constant. Although, this misappropriation as a correction factor might be practical, for a safe design of district heating networks a more sophisticated approach is needed.

Therefore, the presented research focuses on the derivation of a new corrective term that is able to describe the influences of a temperature rise on the maximum friction resistance. Analytical and numerical methods are used within these investigations. For practical purposes, it is important to keep the derivation of the needed input parameters simple. Therefore, well-funded correlations and appropriate simplifications may be used.

2. State of the Art

In general, the estimation of the maximum resistance force is based on Coulomb's friction law [2]. Following Coulomb, the maximum shear stress that can be mobilized between the pipe's mantle and the surrounding soil is proportional to the current normal stress. The constant of proportionality is the coefficient of contact friction μ. Neglecting the shear stresses in circumferential direction, the maximum resistance force that soil can exert on the pipeline due to axial relative displacement can be calculated from equation 1, wherein

$$F_N' = \sigma_0 * \pi * D_a * \frac{1 + k_0}{2} .$$
(2)

Herein D_a denotes the outer diameter of the pipeline and k_0 is the coefficient of earth pressure at rest. Assuming the groundwater level to be beneath the bottom of the pipeline, the overburden stress at the centre of the pipeline is considered as the average normal stress σ_0:

$$\sigma_0 = \gamma * H .$$
(3)

The second term in brackets (equation 1) denotes the sum weight force of the pipeline:

$$F_G' = 2 * \pi * r_m * s * \gamma_s + \pi * r_i^2 * \gamma_w ,$$
(4)

where r_m and r_i are the mean and the inner radius of the medium pipe, respectively. The wall thickness is denoted with s and γ_s and γ_w are the steel and water unit weights. This calculation procedure was proposed by *Rumpel* [3]. He assumes the angle of contact friction φ'_c to be solely dependent on the angle of internal friction φ':

$$\varphi'_c = 0.8 * \varphi' .$$
(5)

For the coefficient of earth pressure at rest he uses *Jaky*'s formula [4]:

$$k_0 = 1 - \sin(\varphi') .$$
(6)

Gramm [5] recommended an increased coefficient of earth pressure, resulting from the densification process during the installation of the pipeline. Values between $0.5 < k_0 < 0.85$ are proposed, dependent on the intensity of densification.

The dependency of the maximum friction resistance on the medium temperature was investigated in full scale field tests by *HEW* (1987) [6]. Two DN700 pipelines of 19.65m length were installed and tested under different thermal conditions. Overburden heights of 0.8m and 1.15m were realized. Within 57 tests a dependency on medium temperature as well as on ambient temperature was observed. The maximum friction force at T=136°C medium temperature was about four times greater compared to T=18°C. For comparable ambient temperatures (in the range of 8.5-10.0°C) a correlation between medium temperature and radial pipeline extension was found, as depicted in Figure 1:
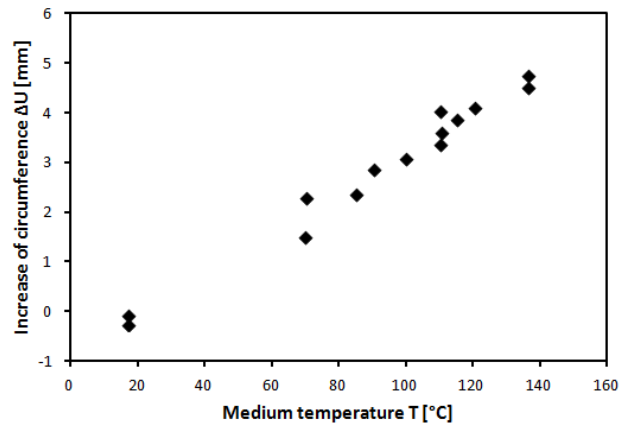

Fig. 1. Dependency of pipeline circumference on medium temperature for DN700 [8].

Further experimental investigations were made by *Gietzelt et al.* (1991) [7]. Pipelines of different diameter were tested in a 25m long trench with concrete walls. For an increase of temperature of ΔT=100K a two times greater resistance force was measured. However, due to the testing conditions, e.g. rigid walls and very high compaction, the practical relevance of their results seems questionable [8].

Huber and Wijewickreme (2014) [9] presented results from experimental tests using a pipeline with an outer diameter of D=520mm. Inside a chamber 3.8m*2.5m*2.5m, pipelines with different medium temperatures were axially displaced until failure. For ΔT=50K an increase of maximum resistance force could be observed. An about 10% higher value was measured, which is only a small increase compared to the aforementioned investigations.

Using analytical and numerical methods, *Achmus* (1995) [8] made investigations in the field of soil-pipeline interaction covering a wide range of topics. Within his investigations on radial pipeline extension, first the ratio between changes of media temperature to mantle temperature was evaluated. Assuming rotational symmetry of heat flux, the mantle temperature was calculated using the method of fictive heat sources and sinks. A thermal conductivity of Λ_S=2.5W/mK for the surrounding soil was found to be in a good agreement with the test results of [6] and [7]. The applied values for the elastic constants E and υ, the thermal expansion coefficient α_t and the thermal conductivity Λ can be found in [8] for the three components of the pipeline. The resulting ratio between changes of media temperature and mantle temperature was found to be between 0.05 and 0.1. In a next step, the radial displacement was evaluated. For the steel pipe and the mantle the theory of thin-walled shells and for the insulation the shell theory in plain strain conditions was considered. The same methodology was also used by *Beilke* (1993) [10].
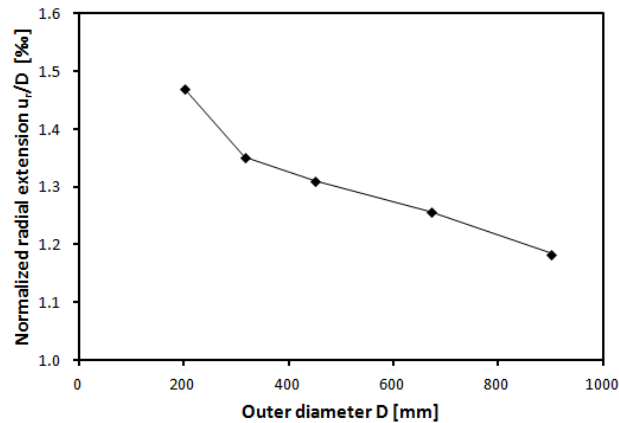
Fig. 2. Normalized radial extension dependent on diameter for ΔT=120K [8].

For an increase of medium temperature ΔT=120K, the radial displacements normalized on diameter are depicted in Figure 2 for different pipeline diameters. Due to the high stiffness of the steel pipe compared to the other materials involved, changes of inner pressure and initial soil stress state were found to have only minor influence on the radial expansion.

Finally a finite element model was established, using the nonlinear elastic Duncan and Chang model [11, 12] to describe the soil behavior. An increase factor κ was introduced, quantifying the increase of maximum resistance force for a medium temperature increase of ΔT=100K. For other thermal conditions, linear inter- and extrapolation is recommended. Within a parametric study was pointed out, that the main influences on κ are the overburden depth h and the deposit density D_r, while the outer diameter has only a minor impact. A functional relation for the increase factor was introduced:

$$\kappa = 1.18 - 0.1h[m] + 1.22D_r\,[1]. \tag{7}$$

3. Numerical model

3.1. General

In order to investigate the impact of a temperature increase on the average radial stress, two-dimensional numerical models were developed using the PLAXIS finite element program [13]. With regard to the symmetry of geometry and loading, only one half of the system was modeled in order to reduce computational effort. Prior to the main analyses, investigations on mesh fineness and model dimensions were made to ensure accurate results. Model dimensions of 18 times the pipeline diameter in horizontal direction and 16 times the diameter in vertical direction, both measured from the pipeline centre, were found to be sufficient. For the developed model, elements with quadratic shape functions were chosen. In contrast to elements with first-order (linear) interpolation, these second-order elements are capable of representing all possible linear strain fields. Additionally the shape approximation of curved structures is much better.
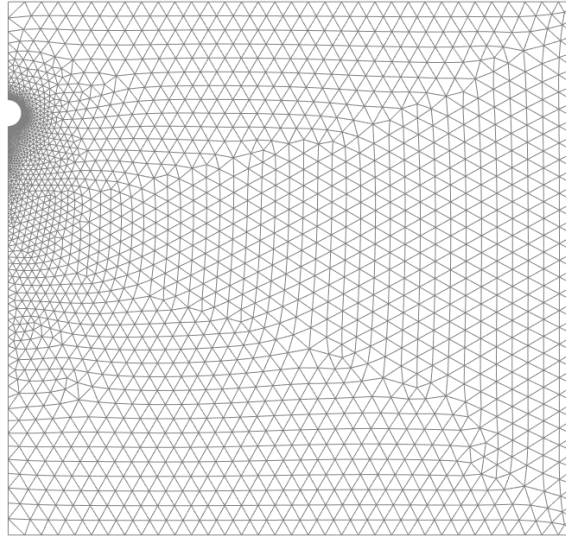
Fig. 3. Exemplary finite element mesh.

Thus, a more accurate solution may be obtained with fewer elements in contrast to first-order elements. The region near the pipe was discretized finer than the far field, where the mesh density can usually be reduced because of lower stress gradients. Figure 3 shows an exemplary finite element mesh.

3.2. Contact model

A relative displacement between the pipe and the surrounding soil occurs under radial or axial pipe displacement. To enable the possibility of relative slipping within the finite element model, a contact condition was defined. The frictional contact was established using the simple friction law according to Coulomb. The classical Coulomb's friction law considers the stick-slip phenomenon, which describes the transition between stick and slip states, depending on the magnitude of applied contact pressure.

An important parameter for the determination of friction forces is the coefficient of friction. In the terminology of soil mechanics the coefficient of friction is written as:

$$\mu = \tan(\varphi'_c),$$ (8)

wherein φ'_c is the angle of contact friction. According to *Rumpel* [3], it is solely dependent on the angle of internal friction (compare equation 5). This equation has not been confirmed by theoretical or experimental investigations. *O'Rourke et al.* [55] carried out 450 laboratory tests, from which an influence of the shore hardness H_D on the angle of contact friction was inferred:

$$\varphi'_c = (-0.0088H_D + 1.15) * \varphi'.$$ (9)

The value of H_D for the commonly used HD-Polyethylene material is in the range of 58 to 62 [14]. With increasing shore hardness, the amount of penetration of the soil particles into the HDPE material decreases, leading to a deterioration of interlocking effects and thus to a decrease in the angle of contact friction. Generally, the proposed values according to this approach are smaller than the ones given by *Rumpel*. Another influence on the angle of contact friction is the relative density D_r. From experiments, *Achmus* [8] determined the following dependency:

$$\varphi'_c = 8.0D_r + 20.0.$$

(10)

Experiments by *Weidlich* (2008) [14] confirmed the dependence on relative density, resulting in the relation:

$$\varphi'_c = 3.0 D_r + 22.3 .$$

(11)

Weidlich chose medium sand with a rounded grain shape, which is representative for commonly used fill material. Therefore, in the following, equation 11 is considered for the determination of the coefficient of contact friction.

3.3. Constitutive model

For the prediction of material behavior using the finite element method, mathematical equations are needed. These so called constitutive equations should describe the stress-strain relationships for any possible problem. However, in contrast to balance equations, which describe physical laws exactly, constitutive equations can only approximate the mechanical behavior. Even if only noncohesive soil is taken into account, numerous constitutive models of different complexity exist. Since complexity is usually associated with many input parameters, which are in practice hard to evaluate, choice has been made for the *Hardening Soil model*.

The *Hardening Soil model* (HS-Model) is an advanced material model for sand. On the basis of *Vermeer* [15], it was developed by *Schanz* [16, 17]. It is formulated in the framework of the classical theory of elastoplasticity. Here, it is assumed that the strain tensor can be decomposed in elastic and plastic components. A yield criterion, stated with the use of a yield function, defines the limit state between purely elastic behavior and the appearance of plasticity. The elastic law describes the stress-strain-relation in the elastic region of the material. Additionally, a plastic flow rule, defining the evolution of the plastic strain, and, if any kind of hardening is taken into account, a hardening law characterizing the evolution of the yield limit has to be formulated. The HS-Model uses a Mohr-Coulomb failure criterion, which involves the cohesion c' and the angle of internal friction φ'. Using the hyperbolic relationship postulated by *Duncan and Chang* [11] the axial strain ε_1 is related to the differential stress q, controlled by the secant modulus E_{50} (figure 4 left):
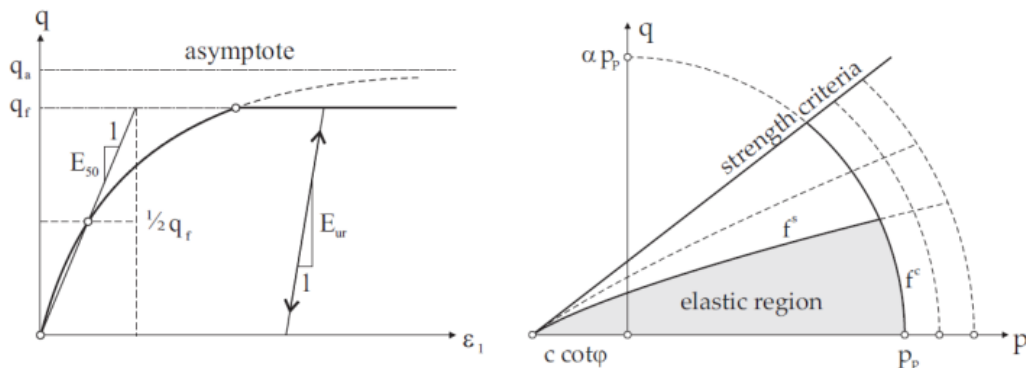

Fig. 4. Hyperbolic stress-strain relation (left) and yield surfaces of the HS-Model (right) [21].

Stiffness parameters are defined for primary loading as well as for un- and reloading. The moduli E_{50} and E_{ur} can be derived from triaxial testing. They are both determined to be stress dependent, which is also true for the oedometric stiffness E_{oed}. To take the stress dependency into account, the power laws of *Janbu* [18] and *Ohde* [19] are used. Another feature of the *Hardening Soil model* is the incorporation of hardening. Hardening is characterized by a dependence of yield stress level on the history of plastic straining [20]. As a result, the yield surfaces are not fixed in principal stress space and, thus, can expand from the initial state (Figure 4 right). In the HS-Model two types of hardening are distinguished: shear and compression hardening, resulting from deviatoric primary loading and isotropic primary loading, respectively. Both types of hardening consider the occurrence of irreversible strains. In this form, the HS-Model needs eight input parameters. All of them can easily be derived from standard laboratory tests.

An extension of the model, termed *HSsmall model*, was developed by *Benz* [21] and is able to account for strain dependency of soil stiffness. An increased stiffness in small strain regions is already known from dynamic analyses. However, this stiffness is mainly dependent on the magnitude of applied strain, not on strain rate [21]. To take this phenomenon into account, the soil stiffness for small shear strains($\gamma < 10^{-6}$), is defined by the small-strain shear modulus G_0. To describe the stiffness degradation with shear strain, a relationship formulated by *Santos & Correia* [25] is implemented in the *HSsmall model*:

$$G/G_0 = (1+0.385*|\gamma/\gamma_{0.7}|)^{-1}.$$ (12)

The parameter $\gamma_{0.7}$ denotes the shear strain at which the shear modulus G is reduced to 72.2% of its initial value G_0. A value of $\gamma_{0.7} = 10^{-4}$ is common practice [13]. Together with these two additional parameters, the HSsmall model requires a total number of ten parameters. Because usually, during the design process of district heating networks, only limited field data are available, a simplified determination process comes into use. In PLAXIS, all four stiffness moduli have to be defined for a reference stress p_{ref}.

$$E_{oed} = E_{oed,ref} * (\sigma_1/p_{ref})^m$$

$$E_{50} = E_{50,ref} * (\sigma_3/p_{ref})^m$$

$$E_{ur} = E_{ur,ref} * (\sigma_3/p_{ref})^m$$ (13)

$$G_0 = G_{0,ref} * (\sigma_3/p_{ref})^m$$

In all calculations the pipe centre level is used as reference and therefore the vertical stress in this depth is assigned as reference stress p_{ref}. To determine the oedometric stiffness modulus at reference stress Eoed,ref, the empirical power law of *Ohde* [19] comes into use, which is well-funded and often used in engineering practice:

$$E_S = \kappa * 100kPa * (\sigma_m/100kPa)^\lambda.$$ (14)

σ_m denotes the mean principal stress. Note that the inherited reference stress of 100kPa is defined within Ohde's power law and should not be mistaken with p_{ref} from the HSsmall model. A bandwidth for the parameters κ and λ, dependent on soil type and relative density, can be found in [1]. It is obvious that the stiffness exponents λ and m have the same meaning and can therefore be used analogous. Because $\sigma_1 = p_{ref}$ at reference depth, no further conversion is necessary and it follows:

$$E_{oed,ref} = E_S.$$ (15)

Within experimental investigations on different sand types, Schanz and Vermeer [22] observed a correlation of the normalized oedometric stiffness modulus $E_{oed,n}$ and the normalized secant stiffness modulus in drained triaxial tests $E_{50,n}$:

$$E_{oed,n} = E_{50,n}.$$ (16)

Note that in [22], the normalization for the oedometric stiffness modulus was done with respect to the major principal stress σ_1, while the secant stiffness modulus was normalized on σ_3. Since we used σ_1 as reference stress p_{ref}, a simple conversion must be done:

$$E_{50,ref} = E_{oed,ref} * \left(\frac{\sigma_3}{\sigma_1}\right)^\lambda.$$ (17)

In initial configuration the major and minor principal stresses are related by the coefficient of earth pressure at rest ($\sigma_3 = \sigma_1 * k_0$). Substitution of σ_3. leads to:

$$E_{50,ref} = E_{oed,ref} * k_0^\lambda.$$ (18)

For completeness, the reference stiffness for un- and reloading $E_{ur,ref}$ must be assigned. Schanz and Vermeer [22] suggest a value of five, while Plaxis [13] recommends a value of three times the reference secant stiffness modulus. Because this parameter is of minor interest for the given problem, the following ratio seems appropriate:

$$E_{ur,ref} = 4 * E_{50,ref} .$$ (19)

For the small-strain shear modulus $G_{0,ref}$. a relation given by *Hardin & Black* [23] is considered:

$$G_{0,ref} = 33 * \frac{(2.97 - e)^2}{1 + e} [MPa] .$$ (20)

This equation is valid for a reference stress of 100kPa and has therefore to be adopted using equation 13. The parameter e denotes the void ratio. Assuming a particle density of 2.65kg/dm³, the void ratio can be determined from the soil unit weight γ.

Beside the stiffness parameters, shear parameters have to be assigned. For the angle of internal friction φ', the recommendations from the AGFW guideline [1] can be used. Thereby, consistency with the soil unit weight γ and the stiffness coefficients κ and λ is ensured. According to *Schanz* [24], the angle of dilatancy ψ' can be correlated with the angle of internal friction:

$$\psi' = \varphi' - 30° .$$ (21)

The parameter sets used in this investigation are summarized in Table 1. To obtain the input parameters for the *HSsmall model*, the described simplified procedure comes into use. This set is completed by the poisson's ratio of $v = 0.25$, as it is common practice for sand, and a cohesion yield stress of c'=0.1kN/m² for the sake of numerical robustness.

3.4. Calculation steps

Each calculation was divided in three steps. In the first step the geostatic stress state was calculated, followed by the installation step, where the pipeline was added to the model. The pipeline was modeled *wished-in-place*, so that effects from the installation process were only approximately considered by the increased value of k_0. The pipeline was fixed in vertical direction and also its self weight was neglected. So, in comparison with equation 1, only the evolution of the term F_N' was investigated within the final step. Herein, a radial displacement was incrementally applied until the diameter dependent final value according to Achmus [8] (Figure 2) was reached. These values represent a temperature increase of ΔT=120K. For the evaluation of the average radial stress σ_r, the contact stresses of the soil-pipeline interface were considered.

Table 1. Soil parameters used in numerical investigations.

Description	Unit weight γ (kN/m³)	Friction angle φ' (°)	Stiffness parameter κ (-)	Stiffness parameter λ (-)	Coefficient of earth pressure k_0 (-)
Dense	19	35	700	0.55	0.75
Medium dense	18	32.5	475	0.65	0.65
Loose	17	30	250	0.75	0.55

4. Parametric study

Within the parametric study, a total number of 45 calculations were performed. In this section, the results are presented, showing impacts of geometric properties, relative density and magnitude of temperature increase.

4.1. Influence of medium temperature

To investigate the impact of a temperature rise on the average radial stress, a normalized description is introduced. Therefore the normalized temperature increase ΔT_{norm}:

$$\Delta T_{norm} = \frac{\Delta T[K]}{120K},$$ (22)

and the normalized increase factor of average radial stress due to medium temperature f_T:

$$f_T = \frac{f_I}{f_{I,(\Delta T=120K)}},$$ (23)

were defined. The factor f_I denotes the ratio of actual average radial stress to its value at initial state. In Figure 5, the results of a reference system are depicted. They are representative for the whole parametric study. For small temperature
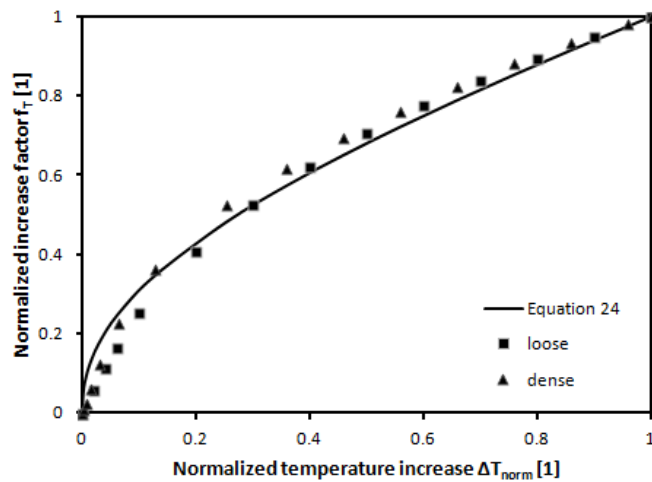

Fig. 5. Normalized description of temperature dependency (DN200, h=3m)

rises, the higher soil stiffness, resulting from the small-strain extension of the HS-model becomes obvious. In consequence, a nonlinear approximation, using a hyperbolic sine function, was chosen:

$$f_T = \frac{\sinh(\Delta T_{norm}^{0.45})}{\sinh(1)}.$$ (24)

A value of 0.45 for the exponent was found to give the best agreement with regard to all investigated models.

4.2. Influence of diameter

As a first geometric property, the pipelines diameter was varied in the range of D=0.2m (DN100) and D=0.9m (DN700). Since medium dense is the relative density with the highest practical relevance, these results are shown in figure 6.
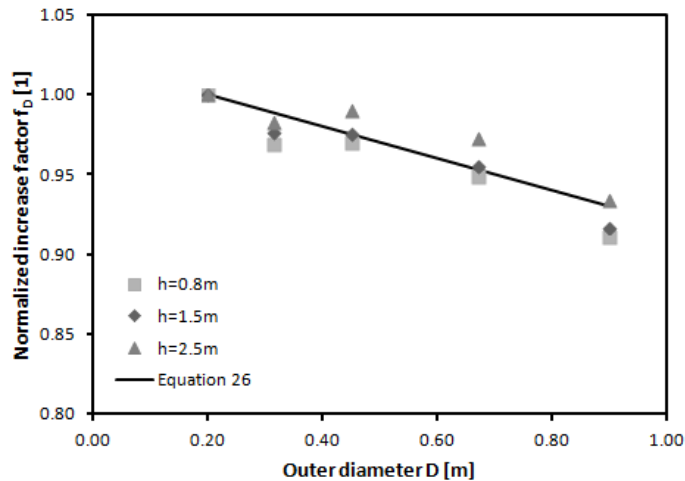

Fig. 6. Normalized description of diameter dependency for medium dense sand

The factor f_D is again a normalized value:

$$f_D = \frac{f_I}{f_D(D = 0.2m)} .$$

(25)

All results belong to the final increase of temperature ΔT=120K. Despite small deviations, a linear regression seems appropriate to approximate the effect of diameter:

$$f_D = 1.02 - 0.1 * D[m] .$$

(26)

4.3. Influence of overburden height

The second geometric parameter under investigation is the overburden height h. For the sake of clarity, and to evaluate the reference increase factor $f_D(D = 0.2m)$, results of different overburden height were written in their corrected form with respect to the outer diameter:

$$f_D(D = 0.2m) = \frac{f_I}{f_D} .$$

(27)

Herein, f_D was calculated according to equation 26. As can be seen from Figure 7, the reference increase factor decreases almost linear with overburden height.
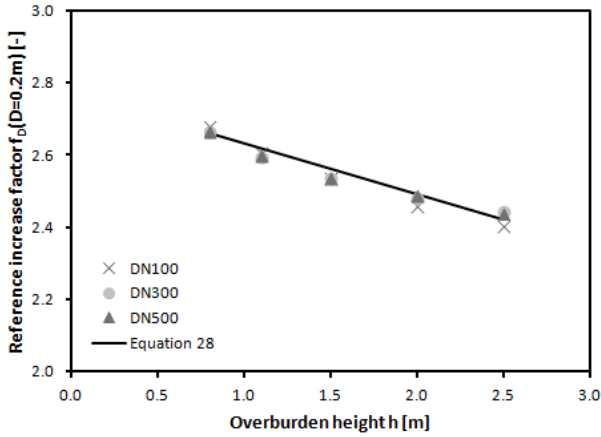
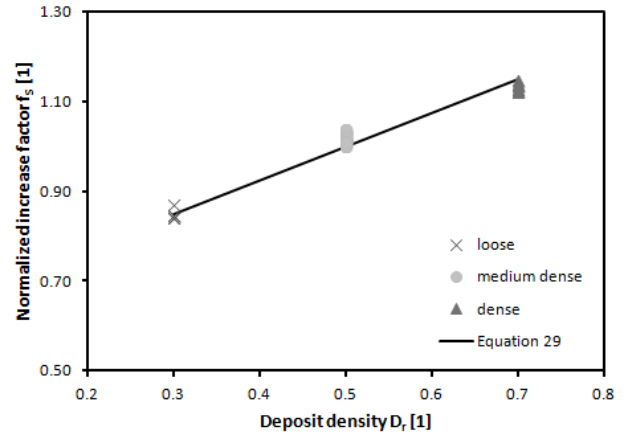Fig. 7. Reference increase factor for different overburden heights

Figure 8. Influence of relative density of sand

Thereby, a good agreement can be achieved with the following relation:

$$f_D(D = 0.2m) = 2.7 - 0.135 * h[m].$$ (28)

So, concerning the impacts of geometry, we can conclude that both, influence of diameter and overburden height, can adequately be described by the presented equations.

4.4. Influence of relative density

Although medium dense sand is commonly used as backfill material within the trench, the relative density was varied in a wide range to define upper and lower limits. The results are depicted in Figure 8. Herein, overburden heights of h=0.8m, 1.5m and 2.5m as well as the nominal diameters DN100, DN300 and DN500 are inherited. Therefore, the geometrically corrected increase factor f_S was plotted over deposit density (cf. Figure 8). The following equation takes different relative densities into account:

$$f_S \equiv \frac{f_I}{f_D * f_D(D = 0.2m)} = 0.625 + 0.75 * D_r$$ (29)

Thereby, the main influences within the scope of work were considered.

4.5. Derivation of a corrective term

In this section, explanation is made how the derived correction terms can be used to determine the increase factor for different boundary conditions. If, e.g. for pipeline design, only the maximum increase of average radial stress is of interest, the increase factor can be calculated in the following way: The overburden height dependent reference value according to equation 28 has to be evaluated and multiplied with the factor for diameter correction (eq. 26) and, if other than medium dense sand is considered, with the correction term for deposit density (eq. 29):

$$f_T(\Delta T = 120K) = f_D(D = 0.2m) * f_D * f_S.$$ (30)

If, in addition, the evolution of the increased radial stress due to an arbitrary temperature rise should be evaluated, equation 24 must be incorporated:

$$f_I(\Delta T) = f_T(\Delta T = 120K) * f_T - f_T + 1.$$ (31)

To verify the accordance of the proposed procedure compared to the results gained from the finite element model, a DN700 pipeline embedded in medium dense sand was investigated (Figure 9). A very good accordance between the finite element solution and the proposed derivation approach can be stated.
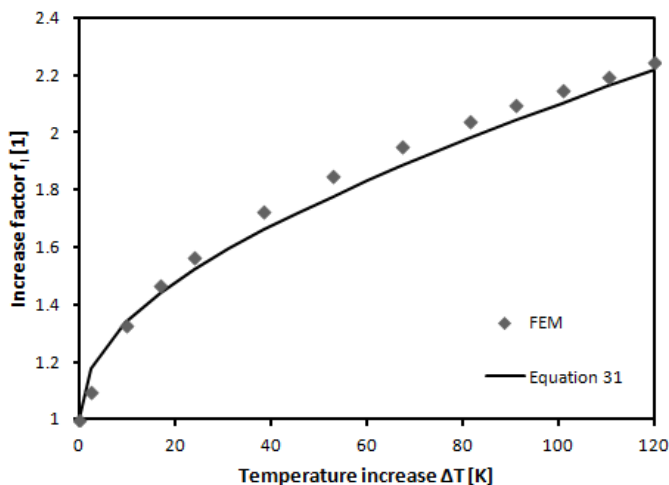

Figure 9. Comparison between FEM und proposed procedure (DN700, h=2.5m, medium dense sand)

5. Conclusions

Within the paper at hand, the influence of medium temperature increase on the average radial stress was investigated. Therefore, after a brief introduction, the state of knowledge concerning this topic was summarized. It can be concluded that, beside few experimental investigations with a limited bandwith of investigated parameters, solely *Achmus* [8] made comprehensive studies on radial pipeline extension. Based on this work, numerous finite element models were developed using the sophisticated *HSsmall model*. Since this model needs numerous input parameters, a simplified derivation procedure was presented. By the use of well-funded correlations, all parameters can be calculated based on empirical values that can be found in the AGFW design code [1].

Within the parametric study, variations of temperature increase, pipeline diameter, overburden height and relative density of sand were carried out. For the dependency on medium temperature, a nonlinear approximation, resulting from the higher stiffness in small strain regions was proposed. The normalization on geometric properties and deposit density could be achieved by the use of linear dependent relations. In agreement with Achmus [8], the overburden height and the deposit were identified to have the strongest influences on the increase factor f_I. The increase factor reaches the highest value for small diameters and overburden heights. As expected, it increases with relative density of sand. A minor impact of the outer diameter was found and therefore considered within the derivation of a corrective term. Qualitatively, the results were similar to *Achmus*. However, the calculated increase factors within this investigation were slightly higher. For medium dense sand, the increase factor was in the range of 1.9-2.3 for a temperature rise of $\Delta T=100K$. As a consequence, significantly higher axial friction resistances must be expected during the operation of district heating networks.

Finally, the use of the developed correction factors was shown for an exemplary model. The agreement between the results gained from the finite element method and the proposed relations were satisfactorily. For the estimation of the maximum friction resistance dependent on medium temperature, the following relation may be used:

$$F_N'(\Delta T) = f_I(\Delta T) * F_N'(\Delta T = 0).$$
(32)

Nevertheless, some simplifications were made and therefore, further research is needed. First, the installation process of the pipeline was only considered roughly. This might be of major impact on the initial state of the surrounding soil. Additionally, a homogenous half space with just one pipeline was modeled, what differs from the field conditions. Another open question is the interdependency with a lateral pipeline displacement, possibly near

arch sections or joints. The latter mentioned is currently under the author's investigation. Incorporating the findings of these investigations, a more reliable design of district heating pipelines should be possible in the near future.

Acknowledgements

References

[1] AGFW e.V.: FW401-10: *"Verlegung und Statik von Kunststoffmantelrohren (KMR) für Fernwärmenetze"*, Frankfurt (2007) *(in German)*.

[2] Coulomb, C. A.: *Essai sur une application des regles des maximis et minimis a quelquels problems de statique relatifs, a la architecture*. In: *Mem. Acad. Roy. Div.Sav.* 7 (1776), p. 343–387 *(in French)*.

[3] Rumpel, G.: *Erdverlegte Verbundrohre für Fernwärme*. In: *Rohrleitungstechnik* (1976), p. 420–434 *(in German)*.

[4] Jaky J.: *Pressure in silos*. 2nd ICSMFE, London (1948), Vol. 1, pp 103-107.

[5] Gramm, G.: *Statik und Festigkeit des Kunststoffmantelrohres*. In: 3R International Jg. 22, Nr.7/8 (1983), p. 355–357 *(in German)*.

[6] HEW, *Fernwärmetransportleitung Karoline-Wedel Kunststoffmantelrohr DN 700*, final report (1987), *unpublished*.

[7] Gietzelt, M.; Engelhardt, H.; Mantley, W.; Grage, T.: *Ermittlung der Reibungskräfte an erdverlegten wärmeführenden Leitungen zur Sicherstellung wirtschaftlicher Konstruktionen*, final report (1991) *(in German)*.

[8] Achmus, M.: *Zur Berechnung der Beanspruchungen und Verschiebungen erdverlegter Fernwärmeleitungen*, PhD thesis (1995), Universität Hannover *(in German)*.

[9] Huber, M.; Wijewickreme, D.: *Thermal Influence on Axial Pullout Resistance of Buried District Heating Pipes*, 14th International Symposium on District Heating and Cooling (2014), Stockholm, Sweden.

[10] Beilke, O.: *Interaktionsverhalten des Bauwerks "Fernwärmeleitung-Bettungsmaterial"*, PhD thesis (1993), Universität Hannover *(in German)*.

[11] Duncan, James M., and Chin-Yung Chang. "Nonlinear analysis of stress and strain in soils." *Journal of the soil mechanics and foundations division* 96.5 (1970): 1629-1653.

[12] Duncan, James M. "Hyperbolic stress-strain relationships." *Application of Plasticity and Generalized Stress-Strain in Geotechnical Engineering*. ASCE, 1980.

[13] Brinkgreve, R.B.J.; Engin, E.; Swolfs, W.M.: PLAXIS 2D 2013 Manual.

[14] Weidlich, I.: *Untersuchung zur Reibung an zyklisch axial verschobenen erdverlegten Rohren*, PhD thesis (2008), Universität Hannover *(in German)*.

[15] Vermeer, PA: *A double hardening model for sand*. In: *Geotechnique* 28 (1978), Nr. 4, S. 413–433.

[16] Schanz, T; Vermeer, PA; Bonnier, PG: *The hardening soil model: formulation and verification*. In: *Beyond 2000 in computational geotechnics* (1999), S. 281–296.

[17] Schanz, T: *Zur Modellierung des mechanischen verhaltens von Reibungsmaterialien*, PhD thesis (1998), Universität Stuttgart *(in German)*.

[18] Janbu, Nilmar: *Soil compressibility as determined by oedometer and triaxial tests*. In: European Conference on Soil Mechanics and Foundation Engineering Bd. 1 (1963), S.19–25.

[19] Ohde, Johannes: *Zur Theorie der Druckverteilung im Baugrund*. (1939) *(in German)*.

[20] Souza Neto, Eduardo A. ; Peric, Djordje ; Owen, David Roger J.: *Computational methods for plasticity: theory and applications*. John Wiley & Sons (2011).

[21] Benz, Thomas: *Small-strain stiffness of soils and its numerical consequences*, PhD thesis (2007), Universität Stuttgart.

[22] Schanz, T. and P. A. Vermeer: *On the stiffness of sands*, Géotechnique 48 (1998): 383-387.

[23] Hardin, Bobby O., and William L. Black. "Closure on vibration modulus of normally consolidated clay." *Journal of Soil Mechanics & Foundations Div* (1969).

[24] Schanz, T, and Vermeer, P.A.: *Angles of friction and dilatancy of sand*, Géotechnique 46 (1996): 145-151.

[25] Dos Santos, J. A., and A. G. Correia: *Reference threshold shear strain of soil. Its application to obtain an unique strain-dependent shear modulus curve for soil*. Proceedings of the Fifteenth International Conference on Soil Mechanics and Geotechnical Engineering, Istanbul, Turkey, 27-31 August 2001. Volumes 1-3. (2001).